Thermal properties in surface-tension-driven convection

C. Pérez-García,[1] B. Echebarria,[1] and M. Bestehorn[2]
[1]*Departamento de Física y Matemática Aplicada, Facultad de Ciencias, Universidad de Navarra, 31080 Pamplona, Navarra, Spain*
[2]*Institut für Theoretische Physik und Synergetik, Universität Stuttgart, Pfaffenwaldring 57/IV, 70550 Stuttgart, Germany*
(Received 17 December 1996; revised manuscript received 21 May 1997)

We discuss the approximations that may be applied to the convective problem of a horizontal layer of liquid in contact with an air layer, both enclosed between conducting walls. Assuming that heat flows across the air mostly by conduction (*conducting-air hypothesis*) the two-fluid problem reduces to the usual Bénard-Marangoni (BM) problem provided the spatial variations of the temperature in the thermal boundary conditions are considered. This approximation is the minimal model to compare with well-controlled BM experiments. The form of the average temperature profiles suggests the reference temperature that ought to be taken in nondimensional parameters that describe these phenomena. We also discuss how the Biot number could be estimated from the Nusselt number and the interfacial temperature field measurements even far from convective threshold. A linear stability analysis is performed with the correct thermal boundary condition. It gives thresholds that slightly differ from those obtained previously. These values are compared with recent experimental findings. All these facts will be useful in performing weakly nonlinear analyses and in planning future experiments on this instability. [S1063-651X(97)10212-4]

PACS number(s): 47.27.Te, 47.20.Dr, 44.25.+f, 47.20.Ky

I. INTRODUCTION

Convective cells, first described by Bénard [1] almost a century ago, are still the paradigm of pattern-forming systems. Since the work by Pearson [2], we know that these cells are mainly due to temperature-induced surface tension gradients at the open upper surface. Under normal conditions, this effect is mixed with buoyancy, leading to the so-called Bénard-Marangoni (BM) convection. [Pure buoyancy convection is known as Rayleigh-Bénard (RB) convection.] Theoretical instability thresholds were determined by Pearson [2] for pure thermocapillary effects and generalized by Nield [3] for the full BM problem.

The main drawback in BM convection is the determination of the heat transfer across the upper free surface, i.e., between the liquid layer and the surrounding air. In most papers the general problem is reduced to a model for the liquid layer (*one-fluid model*), provided the exchanges with air are included in a suitable thermal boundary condition. Usually Newton's law of cooling is assumed, with a constant heat transfer coefficient at the liquid-air interface. However this condition is only satisfied when the interfacial temperature is uniform, i.e., when convection is absent. In other papers it has been argued that this law can be used if heat losses are purely radiative (''vacuum assumption'') [4]. Otherwise, phenomenological values of the heat transfer coefficient can be used to reach an order-of-magnitude comparison between theoretical values and experiments involving an air layer over the free liquid surface [5].

But within the one-fluid model the measurement of the temperature at the interface is a delicate experimental problem. In effect, in this model the control parameter would be the temperature difference between the bottom plate and the interface. Some authors have tried to estimate the interfacial temperature with local probes (thermocouples and thermistors) in some experiments. But these probes have some inconveniences: (a) they provide only local measurement of an interfacial field, (b) they always modify the interface, and (c) they only provide approximate values [6]. Other authors have suggested using a suitable ''average'' of the ambient air [7] temperature, but such a criterion has some arbitrariness and cannot be considered for quantitative comparisons.

The BM instability is intrinsically a two-fluid problem [8]. The two-fluid problem is mathematically much more involved than the one-fluid model. The main purpose of the present paper is to perform a consistent reduction from the two-fluid model to the one-fluid model, using suitable approximations, mainly the disparity between air and liquid properties. We will see that a consistent reduction consists in assuming that air transfers heat by conduction only (conducting-air hypothesis). In order to discuss such a minimal model we will review the evolution equations and the boundary conditions of this problem, and then we will proceed to discuss the thermal properties of the system. Some attention is paid to the discussion of the temperature difference that should be taken to determine the value of nondimensional parameters. We compare the results of the conducting-air hypothesis with the classical ones due to Pearson [2] and Nield [3]. Finally we present a comparison of these results with the most remarkable experimental results on convective thresholds in BM convection.

II. MECHANICAL BOUNDARY CONDITIONS IN THE TWO-FLUID BM INSTABILITY

Let us review briefly the main characteristics of the setup used in recent experiments, in which excellent thermal control has been achieved [9–11]. This consists of a liquid layer of thickness d_l on a rigid conductive plate attached to a heater. The power of the heater is adjusted in order to keep the temperature fixed at the bottom. A thin air layer of thickness d_a is enclosed between the liquid and a rigid conducting lid. Usually this lid is a sapphire window that allows optical measurements. Its bottom is in contact with the air and its

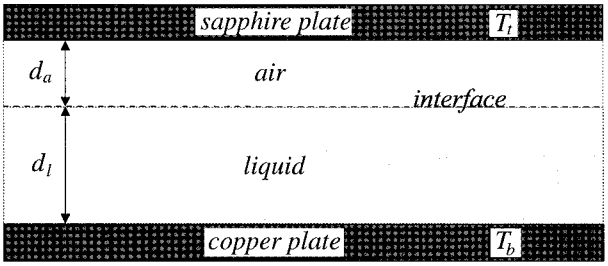

FIG. 1. Diagram of the setup to study Bénard-Marangoni convection.

top with a refrigeration bath. The circulation through the bath carries heat away while keeping the temperature T_t of the sapphire constant. When the temperature at the bottom plate T_b is raised sufficiently one passes from a conductive state to convection. Thus the main control parameter is the total temperature difference $\Delta T_T = T_b - T_t$ across the two layers. (For simplicity, we do not consider the temperature drops in the bottom plate and the sapphire lid.) A diagram of this configuration is shown in Fig. 1.

For small heating the evolution equations (continuity, momentum balance, and energy balance equations) have a purely conducting (quiescent) solution:

$$\mathbf{v}_l = \mathbf{0}, \quad T_l(z) = T_b - \frac{\Delta T_l^c}{d_l} z \quad (0 < z < d_l), \tag{1}$$

$$\mathbf{v}_a = \mathbf{0}, \quad T_a(z) = T_t - \frac{\Delta T_a^c}{d_a} [z - (d_l + d_a)] \quad [d_l < z < (d_l + d_a)], \tag{2}$$

where ΔT^c stands for the conductive temperature difference across the liquid and the air, respectively, $\mathbf{v}$ denotes the velocity, and the subscripts indicate values in the air (a) and in the liquid (l), respectively. This is the reference state which is stable for small heating. Perturbations around this state (small or finite) evolve according to similar equations, supplemented with suitable boundary conditions (BC). On rigid conducting plates,

$$\mathbf{v}_l = \mathbf{0}, \ \theta = 0 \quad \text{at } z = 0, d_l + d_a, \tag{3}$$

where θ is the temperature perturbation.

Bénard [1] reported interfacial deflection measurements, but deviations from flatness are at most about $10^{-3} d_l$ (hereafter we will assume $d_l \simeq 1$ mm). [However, in thin layers ($d_l \leqslant 0.3$ mm) deflection makes an essential, non-negligible contribution [12].] Here, we will suppose that the interface is flat, undeformable.

In normal liquids the higher the temperature is the smaller is the surface tension σ, i.e., $\sigma = \sigma_0 (1 - |d\sigma/dT| \theta)$. Therefore, the mechanical BC, which states continuity of tangential stresses, leads to

$$v_z = 0 \tag{4}$$

$$\mu_l \partial_z v_x|_l - \mu_a \partial_z v_x|_a = |d\sigma/dT| \partial_x \theta, \tag{5}$$

$$\mu_l \partial_z v_y|_l - \mu_a \partial_z v_y|_a = |d\sigma/dT| \partial_y \theta. \tag{6}$$

Continuity requires some motion in the air layer, because $\mathbf{v}_l \neq \mathbf{0}$ implies $\mathbf{v}_a \neq \mathbf{0}$ at the interface. On the other hand, $\partial_z \mathbf{v}_a$ may be of the same order as $\partial_z \mathbf{v}_l$. As $\mu_l \gg \mu_a$, the air terms in Eqs. (5) and (6) can be dropped. Hence the mechanical BC reduces to

$$\mu \partial_z v_x = |d\sigma/dT| \partial_x \theta, \tag{7}$$

$$\mu \partial_z v_y = |d\sigma/dT| \partial_y \theta, \tag{8}$$

which after applying the continuity equation reads

$$\partial_z^2 v_z|_l = \frac{|d\sigma/dT|}{\mu_l} \nabla_h^2 \theta, \tag{9}$$

where ∇_h^2 is the horizontal Laplacian operator.

Equations (3), (5), (6), (9), and (10) make up a complete set of BC for the BM instability problem, where two main approximations have been applied: (a) the interface is assumed to remain flat and (b) viscous effects in the air are negligible in comparison with those in the liquid. In the next section we discuss the approximations which determine the thermal BC.

III. HEAT TRANSFER ACROSS THE UPPER FREE SURFACE

Now we recall the thermal BC. Continuity of temperature and heat flux across the interface leads to the following thermal BC:

$$T_l = T_a, \ \theta_l = \theta_a, \ q_{zl} = q_{za}, \tag{10}$$

q_z being the vertical component of the heat flux. At a steady flat interface the last condition reads $\lambda_l \partial_z T_l = \lambda_a \partial_z T_a$ (λ is the heat conductivity).

The reduction from the two-fluid problem to the one-fluid model always involves some hypothesis on the thermal BC at the interface. Usually it is assumed that the air layer is quiescent and that the heat flow from the liquid to the air obeys Newton's cooling law with a constant coefficient h. Under this hypothesis Eq. (10) becomes

$$\partial_z \theta_l = -h \theta_l. \tag{11}$$

In early experiments the value of h was set as an adjustable parameter for comparison with theoretical thresholds. This procedure is arbitrary and does not allow determination of precise values for this parameter.

This procedure can be improved by examining the temperature profiles across the two fluids in different situations. As a reference, let us consider Rayleigh-Benard convection between two rigid plates. The experimental setup includes bottom and top plates with higher thermal conductivities than the convective fluid, to keep the temperatures fixed in both plates. When convection begins, the linear temperature profile is modified by increasing the mean temperature gradient at the boundaries, then decreasing it in the midregions of the fluid, as sketched in Fig. 2 [13]. In BM convection the temperature and heat flux perturbations are linked at the boundary. For small ΔT, there are two linear conductive

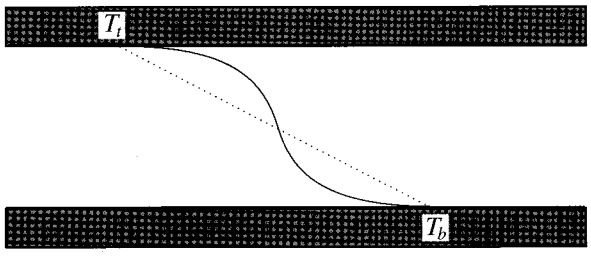

FIG. 2. Diagram of the temperature profiles in Rayleigh-Bénard convection between conducting plates. The dotted line indicates linear conductive profiles, while the solid one represents convective profiles.

profiles, one across the liquid and another through the air, as sketched in Fig. 3. The slopes of these profiles are obtained from the thermal BC Eq. (10):

$$\lambda_l \frac{T_b - T_i^c}{d_l} = \lambda_a \frac{T_i^c - T_t}{d_a}, \tag{12}$$

which fixes in a unique way a reference interfacial temperature T_i^c as a function of T_b and T_t (see Fig. 3). (The superscript c indicates that the reference temperature is obtained from a conductive profile.) Now we assume that a perturbation θ acts on the conductive profile, so that $T_i = T_i^c + \theta$, and the thermal BC Eq. (10) can be written as

$$\lambda_l \partial_z (T_i^c + \theta) = -\lambda_a \frac{(T_i^c + \theta) - T_t}{d_a}. \tag{13}$$

Using Eq. (12) we arrive at Eq. (11), provided h is taken to be

$$h_0 = \frac{\lambda_a}{\lambda_l d_a}. \tag{14}$$

The relationship Eq. (14) is the only point at which the air properties enter the one-fluid model.

But in deriving Eq. (14), θ has been assumed to be spatially uniform, which is not the case. To include spatial dependence of θ the simplest method is to consider heat conduction through the air. The situation is shown schematically in Fig. 3. Once convection becomes stationary in the liquid, the local temperature slope near the bottom is smaller (it is a negative quantity) than in the conductive case. Likewise the linear temperature slope also diminishes in the air layer, thus giving an increment θ to the average temperature. So, to fulfill the thermal BC conditions the local slope near the liquid interface must be smaller than in the conductive case (the term $\partial_z \theta \neq 0$ must be added).

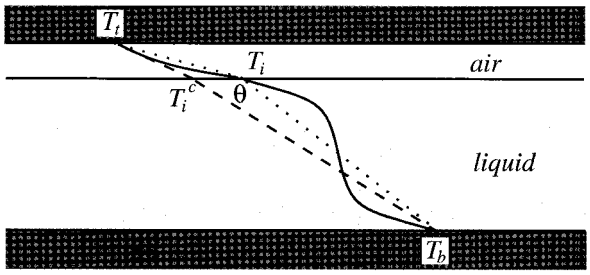

FIG. 3. Scheme of the temperature profiles in a Bénard-Marangoni cell. The dotted line indicates linear conductive profiles through the liquid and through the air. The solid curve represents the profiles in each medium. The curve (temperature) and its derivative (heat flux) must be continuous at the interface. For liquid convection the average interface temperature is modified by a factor $\langle\theta\rangle$. The heat fluxes are also changed accordingly in these circumstances.

Conduction in the air settles between a fixed T_t and a heterogeneous temperature field $T_i^c + \theta(\mathbf{x})$, where $\mathbf{x}$ stand for horizontal coordinates. This fact is considered in expanding the temperature perturbation field in terms of normal modes $\theta(\mathbf{x},z) = \Theta(z)\exp(-i\mathbf{k}\cdot\mathbf{x})$, where $\mathbf{k}$ stands for the horizontal wave number. Then, Laplace's equation results in $\partial_z^2\Theta - k^2\Theta = 0$. Solutions of this equation are of the form $\Theta(z) = A\cosh(kz) + B\sinh(kz)$. Applying the rest of the thermal BC Eq. (10), Newton's cooling law Eq. (11) is recovered, provided the coefficient h is taken as

$$h = \frac{\lambda_a k}{\lambda_l \tanh(k d_a)}. \tag{15}$$

Notice that this is the form expected for the heat transfer coefficient in an insulating plate [14]. In the particular cases $d_a \to 0$ and $k \to 0$, which physically are equivalent to $d_a \ll 1/k$, i.e., the thermal properties of the air layer do not *feel* the spatial structure of the underlying liquid and h reduces to h_0.

Let us discuss now the range of validity of the conducting-air hypothesis. The typical Rayleigh number R for an air layer of $d_a \approx 1$ mm is far smaller than $R_c = 670$ of an incompressible fluid with an open surface, so natural convection in the air is excluded near the onset of convection. On the other hand, continuity drives some motions from the liquid to the air that produce a *forced-convection* contribution to heat transport. The magnitude of this term is estimated by the Peclet number $P = V d_a/\kappa_a$, where V is a typical velocity and κ the heat diffusivity. Since on the interface $V_a = V_l \approx \kappa_l/d_l$, the component of heat transport due to forced convection in the air is smaller than that due to conduction by a factor $P \approx D/K \approx 10^{-2}$ ($D = d_a/d_l$, $K = \kappa_a/\kappa_l$). Moreover, numerical simulations of the two-layer problem confirm that the effective thermal conductivity in the air does not change for small supercriticality [11].

IV. EVOLUTION EQUATIONS AND NONDIMENSIONAL PARAMETERS

What would be the control parameter in the one-fluid model? Usually $\Delta T = T_b - T_i$ would be suggested by a theorist. But with this choice the problem is not well-defined because $T_i = T_i^c + \theta(\mathbf{x})$ is established on the interface. Some kind of horizontal average $\langle\theta\rangle$ should be taken into $T_b - \langle T_i\rangle$ but no technique allows us to measure $\langle\theta\rangle$ without modifying the interfacial properties. Moreover, from inspection of Fig. 3 it is clear that θ is, in general, a two-fluid quantity. These drawbacks suggest the use of a quantity easily related to the control parameter ΔT_T in experiments. In agreement with the conducting-air hypothesis, the conducting temperature difference across the air is subtracted from

ΔT_T and the resulting difference $\Delta T = T_b - T_i^c$ is used as the reference for the temperature (in the next paragraph we will give the relationship between ΔT_T and ΔT). Besides this reference ΔT for temperature we use d_l for length and d_l^2/κ for time. The evolution equations become

$$\boldsymbol{\nabla} \cdot \mathbf{v} = 0, \tag{16}$$

$$\mathrm{Pr}^{-1} d_t \mathbf{v} = -\nabla \pi + \nabla^2 \mathbf{v} + R\theta \mathbf{e_z}, \tag{17}$$

$$d_t \theta + v_z = \nabla^2 \theta, \tag{18}$$

and the boundary conditions become

$$\mathbf{v} = \mathbf{0}, \quad \theta = 0 \quad \text{on} \quad z = 0, \tag{19}$$

$$\partial_z^2 v_z|_l = -M \nabla_h^2 \theta, \quad \partial_z \theta = -\mathrm{Bi}\,\theta \quad \text{on} \quad z = 1, \tag{20}$$

where for simplicity the same notation for nondimensional variables is maintained and the following nondimensional numbers have been introduced:

$$\mathrm{Pr} = \frac{\mu}{\rho \kappa} \quad \text{(Prandtl number)}, \tag{21}$$

$$R = \frac{\rho \alpha g (T_b - T_i^c) d^3}{\mu \kappa} \quad \text{(Rayleigh number)}, \tag{22}$$

$$M = \frac{|d\sigma/dT|(T_b - T_i^c) d}{\mu \kappa} \quad \text{(Maragoni number)}, \tag{23}$$

$$\mathrm{Bi} = h d_l = \frac{\lambda_a k}{\lambda_l \tanh\left(\dfrac{d_a}{d_l} k\right)} \quad \text{(Biot number)}. \tag{24}$$

The temperature difference $\Delta T = T_b - T_i^c$ is not directly measurable but it is derived from ΔT_T by the simple relationship

$$\Delta T = \Delta T_T - (T_i^c - T_t) = \frac{\mathrm{Bi}_0}{1 + \mathrm{Bi}_0} \Delta T_T, \tag{25}$$

where $\mathrm{Bi}_0 = \mathrm{Bi}(k=0)$. Hence the nondimensional numbers M_T and R_T built with the parameter ΔT_T are linked to M and R through

$$(M_T, R_T) = \frac{\mathrm{Bi}_0 + 1}{\mathrm{Bi}_0} (M, R). \tag{26}$$

We complete this section with some comments on the Nusselt number, a dimensionless measure of heat conduction accessible from calorimetric measurements that can be given by $\mathrm{Nu} \equiv \langle q_z \rangle / \langle q_z^c \rangle$ or equivalently $(q_z^c|_l = -\lambda_l [(T_b - T_i^c)/d_l])$

$$\mathrm{Nu} = 1 - \frac{d_l}{T_b - T_i^c} \langle \partial_z \vartheta \rangle \tag{27}$$

(ϑ indicates that the temperature perturbation is taken with its dimensions here). After introducing the thermal BC Eq. (20) and using dimensionless variables, this reads $\mathrm{Nu} = 1 + \langle \mathrm{Bi}(k)\,\theta \rangle$. The horizontal average is equivalent to taking the limit $k \to 0$. Then, with full generality

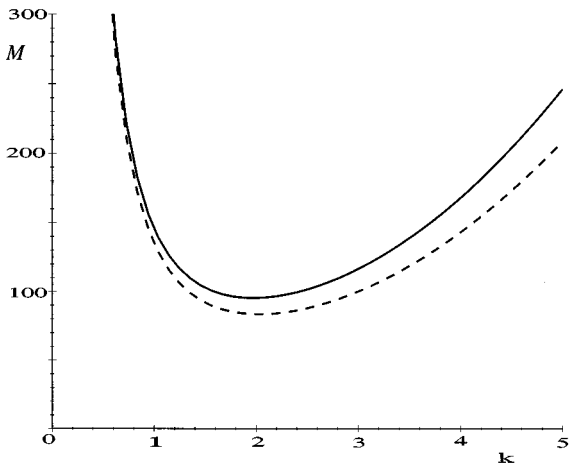

FIG. 4. Marginal curves. The solid curve is for Eq. (29) and the dotted line is the curve resulting from Pearson's results with a constant $\mathrm{Bi} = \mathrm{Bi}_0$. ($\Lambda$ is taken fixed at $\Lambda = 0.204$.)

$$\mathrm{Nu} = 1 + \mathrm{Bi}(k=0) \langle \theta \rangle. \tag{28}$$

Under the conducting-air hypothesis $\mathrm{Bi}(k=0) = \mathrm{Bi}_0$, and the Nusselt number reduces to $\mathrm{Nu} = 1 + \mathrm{Bi}_0 \langle \theta \rangle$. From this last expression it becomes apparent that the perturbation θ holds the whole information on the convective heat transport. This perturbation θ, or equivalently T_i, cannot be determined with local invasive probes like thermocouples or thermistors, but it requires accurate indirect measurements. Regarded as a phenomenological coefficient, $\mathrm{Bi}(k=0)$ can be inferred from calorimetric measurements even far from threshold.

V. CONVECTIVE THRESHOLDS

Now let us seek the consequences of the thermal BC Eq. (20) on the linear stability analysis. Usually, Bi is regarded as constant [2,3], but, in general, $\mathrm{Bi}(k) \geqslant \mathrm{Bi}_0$. Thus, the linear problem becomes a little more cumbersome, though it can be solved without difficulty.

A. The case $R = 0$

The case $R = 0$ (no buoyancy) can be treated analytically. Furthermore, this is the case in which the interfacial contributions give the highest corrections. The marginal curve is simply

$$M(k) = \frac{8k^2 \{1 + [\Lambda \tanh k / \tanh(Dk)]\}(k - \sinh k \cosh k)}{k^3 - \sinh^2 k \tanh k}. \tag{29}$$

Here the air properties appear within the ratios $\Lambda = \lambda_a/\lambda_l$ and $D = d_a/d_l$. The minimum of this curve gives the threshold values M_c and k_c. Figure 4 shows the curve Eq. (29) together with that resulting from taking a constant value $\mathrm{Bi} = \mathrm{Bi}_0$.

The factor $\mathrm{Bi}(k)$ has two effects: (a) it increases the convective threshold M_c, because M_c increases by increasing Bi (see Table I in Ref. [3]) and (b) it shifts the critical wave number k_c. For fixed Λ, $M(k)$ increases monotonically as D increases. Two limiting cases can be distinguished. When

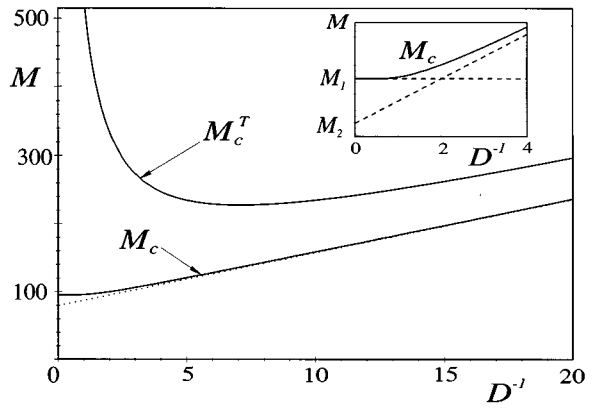

FIG. 5. The critical Marangoni number M_c as a function of $D^{-1}=d_l/d_a$. It tends to the value $M_1=M_{\mathrm{Bi}=k_c\Lambda}$ for small d_l/d_a. Asymptotically it goes like $M=M_2(1+\Lambda/D)$, where $M_2=M(\mathrm{Bi}=k_c\Lambda)$. In the upper curve in this figure $M_{T_c}=(\mathrm{Bi}_0+1)M_c/\mathrm{Bi}_0$ is represented. Its minimum is at $d_a/d_l\simeq 0.15$ for the experiments quoted in Table I. (The same value $\Lambda=0.204$ as in Table I has been taken.)

$D\to 0$ ($d_a\gg d_l$), $M\to M(\mathrm{Bi}=k\Lambda)$, while for $D\to\infty$ ($d_a\ll d_l$), $M\to M(\mathrm{Bi}_0)$. As the most physically interesting case is the latter one, we give the main results in terms of D^{-1}. The critical value M_c is plotted as a function of D in Fig. 5 for a value $\Lambda=0.204$ used in Table I. From curves in that figure it is obvious that corrections given from $\mathrm{Bi}(k)$ are most significant in the range $0.5<D<3$, i.e., when the liquid and air depths are of the same order of magnitude.

In this point it is worthwhile to comment on some unclear results in a recent paper [15]. There, the thermal boundary condition was improperly taken as if the temperature could be kept fixed throughout the air layer, or, equivalently, considering the air to be a good thermal conductor. As a consequence, the temperature profile in that paper [Eq. (2)] is only continuous at the interface in the limiting case of a vanishing air layer ($d_a\to 0$). Furthermore, in this particular limit the main result in that paper [Eq. (10)] is correctly obtained from Eqs. (29) using the relationship between M_T and M deduced in the preceding section. In Fig. 5 the value of the critical M_T as a function of D^{-1} is represented to show that the results of Fig. 1 in Ref. [15] are recovered here as a particular case.

B. The case $R\neq 0$

R is not usually negligible in experiments. In fact, the dimensionless numbers M and R are not independent but are linked through the relationship $\Gamma=M/R=(|d\sigma/dT|)/(\rho\alpha g d_l^2)$. This parameter Γ measures the relative importance of Marangoni and buoyancy effects. (For a given liquid and a fixed depth, the ratio of M and R is fixed.) In thermocapillary-driven experiments, $0<\Gamma^{-1}\leqslant 1$. We performed numerical simulations including this factor and $\mathrm{Bi}(k)$. The main result is that the linear relationship found by Nield [3], $M_c/M_{0c}+R_c/R_{0c}\simeq 1$, is still valid, provided the appropriate values M_{0c} (pure Marangoni, no buoyancy) and R_{0c} (buoyancy alone, no surface-tension variations) are taken. We summarize in Table I the values obtained in this analysis for the experimental value $\Lambda=0.204$ [10] and for several values of Bi_0. (As $D=\Lambda/\mathrm{Bi}_0$ we take Bi_0 as the main parameter to compare with Table I in Ref. [3].) For the sake of comparison the values of Table I in Ref. [3] are also included in this table. In our case a maximum deviation of 3% from this straight line is found for all the values of Γ and D used in experiments. (See also the discussion in Ref. [16].) After using that linear relation and the definition of Γ we obtain an expression valid for any value of Γ,

$$M_c=\frac{\Gamma M_{0c}R_{0c}}{\Gamma R_{0c}+M_{0c}}, \tag{30}$$

which holds with an uncertainty of 3%.

In comparisons between experiments and theory, Bi has been underestimated (a reference value $\mathrm{Bi}\simeq 0.1$ [9,17] was used) or the correction due to $\Gamma\neq 0$ was not included [9,18]. Schatz *et al.* [10] include the last correction and the value of Bi is taken as Bi_0 (conductive heat transport assumption). We quote in Table II the values of three recent experiments together with the results for $\mathrm{Bi}(k_c)$ from our analysis. The value of Γ is easily obtained from the parameter values tabulated in each experiment. The values of M_c and R_c have been calculated from Eq. (30) and Nield's linear relationship with the values of M_{0c} and R_{0c} in Table I. Notice that the $\mathrm{Bi}(k_c)$ differs significantly from the value $\mathrm{Bi}=0.2$ taken by Koschmieder and Switzer [9]. On the other hand, in the case $d_a\simeq d_l$, $\mathrm{Bi}(k_c)$ differs by a factor of 2 from Bi_0, the value taken in Ref. [10]. There is also a discrepancy between the theoretical threshold values of k_c and those obtained in experiments. The main source of discrepancy lies probably in the inaccuracy in the measurements of $d\sigma/dT$ ($\pm 10\%$). In our calculations $k_c=1.97$, which is smaller than the smallest value $k_c=1.99$ ($\mathrm{Bi}=0$) reported by Nield but still higher than the experimental value $k_c=1.90$.

TABLE I. Values of M_{0_c} and R_{0_c} for $\Lambda=0.204$, $D=\Lambda/\mathrm{Bi}_0$, and several values of Bi_0. These values must be compared with those in Table 1 of Ref. [3].

Bi_0	M_{0_c}	k_c	$M_{0_c}^{\mathrm{Nield}}$	k_c^{Nield}	R_{0_c}	k_c	$R_{0_c}^{\mathrm{Nield}}$	k_c^{Nield}
0	95.241	1.970	79.607	1.993	721.65	2.135	669.00	2.088
0.01	95.241	1.970	79.991	1.997	721.65	2.135	670.38	2.089
0.1	95.251	1.971	83.427	2.028	721.66	2.139	682.36	2.117
0.2	95.800	1.992	87.195	2.060	722.84	2.147	694.78	2.144
0.5	102.610	2.096	98.256	2.142	739.80	2.207	727.42	2.212
1	118.540	2.221	116.127	2.246	775.91	2.290	770.57	2.293
2	152.012	2.374	150.679	2.386	833.19	2.391	831.27	2.393

TABLE II. Experimental and theoretical threshold values.

	Oil	d_l	d_a	Γ	Bi_0	Bi (k_c)	M_c^{theor}	M_c^{expt}
Koschmieder	100 cs	3	0.4	0.6	1.2	1.3	100	71
and		1.9	0.4	1.5	0.8	0.8	100	62
Switzer	50 cs	1.9	0.4	1.4	0.8	0.9	100	72
		1.2	0.4	3.5	0.5	0.6	98	61
Schatz *et al.*	7 cs	0.4	0.45	44	0.2	0.4	95	84
Nitschke *et al.*	10 cs	1.41	0.50	2.9	0.6	0.7	99	99

VI. DISCUSSION

Close to the convective threshold, heat flows across the air layer mainly by conduction. This fact allows us to propose a minimal model, which we called the *conducting-air approximation*, in which the real two-fluid problem can be reduced to a one-fluid system, provided that a simple modification of Newton's heating law is made. The constant coefficient in this law must be replaced by a k-dependent coefficient. With this model most of the questions raised in the introduction of a recent work by Parmentier *et al.* [7] can be answered.

We discussed the reference temperature to be used in nondimensional numbers, a point relevant to any comparison between theory and experiments. In this paper we argued that a suitable choice for the reference for the temperature in the dimensional analysis is $\Delta T^c = T_b - T_i^c$, a quantity easily derived from the *external control parameter* ΔT_T in experiments through the simple relation $\Delta T^c = \mathrm{Bi}_0/(\mathrm{Bi}_0+1)\Delta T_T$.

From the general relationship between the interfacial temperature T_i and the Nusselt number $\mathrm{Nu}=1+\mathrm{Bi}(k=0)\langle\theta\rangle$ the coefficient $\mathrm{Bi}(k=0)$ can be determined, even far from threshold, after measuring T_i with a suitable technique and Nu with a calorimetric technique.

A linear stability analysis gives us the convective thresholds under quite general conditions. In the limiting case of no buoyancy (pure Marangoni effect) our results differ by less than 1% from those obtained by Smith [19] considering the whole surface-tension-driven instability (with deflections and convection in air). The general case is also considered and we discuss some practical rules for obtaining the appropriate threshold values. Fortunately the linear relationship $R_c/R_{0c} + M_c/M_{0c} = 1$ found by Nield [3] still holds provided the right threshold values R_{0c} and M_{0c} are used. A comparison with recent experimental thresholds [9,10,18] is also presented. The critical wave number k_c in our analysis ($k_c = 1.97$) is slightly smaller than the smallest value obtained by Nield [3] ($k_c = 1.99$) but still higher than that in experiments ($k_c = 1.90$)

Although the model presented here is strictly valid for small supercriticality, the points raised in this paper must be taken into account in pursuing a nonlinear analysis and, in particular, in fully explaining the striking hexagon-square transition recently discovered in experiments [18,20,21].

From the experimental side, the effects studied in this paper become more important as the air layer is made thinner ($d_a < 0.5$ mm). But d_a cannot be decreased below a wetting value [11]. On the other hand, the thinner the fluid layer d_l, the smaller the buoyancy and the bigger the thermocapillary effect. But the ratio d_a/d_l should be kept as small as possible to minimize the drawback of a k-dependent Biot number. The optimization of these factors may improve the experimental setups used so far. This comment is especially relevant for planning future experiments under microgravity conditions.

ACKNOWLEDGMENTS

This research was supported by the PIUNA (Universidad de Navarra) and the DGICYT-PB95-0578 (Spanish Government). One of us (B.E.) would like to thank the Basque Government for financial support. We are grateful to Professor H. Mancini (Universidad de Navarra) for his collaboration in this research and to Dr. Kolodner (Lucent Technologies, Murray Hill, N.J.) for many useful comments and discussions.

[1] H. Bénard, Rev. Gen. Sci. Pure Appli. **11**, 1261 (1900).
[2] J. R. A. Pearson, J. Fluid Mech. **4**, 489 (1958).
[3] D. A. Nield, J. Fluid Mech. **19**, 341 (1964).
[4] A. Thess and S. A. Orszag, J. Fluid Mech. **283**, 201 (1995).
[5] L. Koschmieder and M. I. Biggerstaff, J. Fluid Mech. **167**, 49 (1986); L. Koschmieder, *Bénard Cells and Taylor Vortices* (Cambridge University Press, Cambridge 1993).
[6] T. E. Hikenbein and J. C. Berg, Int. J. Heat Mass Transf. **21**, 1241 (1978); P. Cerisier, C. Jamond, J. Pantaloni, and C. Pérez-García, Phys. Fluids **30**, 954 (1987).
[7] P. M. Parmentier, V. C. Regnier, G. Lebon, and J. C. Legros, Phys. Rev. E **54**, 411 (1996).
[8] D. D. Joseph and Y. Renardy, *Fundamentals of Two-Fluid Dynamics* (Springer, New York, 1993); I. B. Simanovskii and A. A. Nepomnyashchy, *Convective Instabilities in Systems with Interface* (Gordon & Breach, London, 1993).
[9] L. Koschmieder and D. W. Switzer, J. Fluid Mech. **240**, 533 (1992).
[10] M. F. Schatz, S. J. VanHook, W. D. McCormick, J. B. Swift, and H. L. Swinney, Phys. Rev. Lett. **75**, 1938 (1995).
[11] K. Nitschke, M. Bestehorn, and A. Thess (unpublished).
[12] S. J. VanHook, M. F. Schatz, W. D. McCormick, J. B. Swift, and H. L. Swinney, Phys. Rev. Lett. **75**, 4397 (1995).
[13] W. V. R. Malkus and G. Veronis, J. Fluid Mech. **4**, 225 (1958).
[14] F. H. Busse, J. Fluid Mech. **96**, 243 (1980); M. R. E. Proctor, *ibid.* **113**, 469 (1981).

[15] L. M. Rabin, Phys. Rev. E **53**, R2057 (1996).
[16] L. Hadji, J. Safar, and M. Schell, J. Nonequilib. Thermodyn. **16**, 343 (1991).
[17] J. Pantaloni, R. Bailleux, J. Salan, and M. G. Velarde, J. Nonequilib. Thermodyn. **4**, 201 (1979).
[18] K. Nischke and A. Thess, Phys. Rev. E **52**, R5772 (1995).
[19] K. A. Smith, J. Fluid Mech. **24**, 401 (1966).
[20] M. Bestehorn, Phys. Rev. Lett. **76**, 46 (1996).
[21] M. Schatz, http://chaos.ph.texas.edu/~ schatz/sec_instab.htlm